Contents list available at CBIORE journal website

International Journal of Renewable Energy Development

Journal homepage: https://ijred.cbiore.id

Research Article

Experimental investigation of inter-electrode distance and design in *Cymbopogon citratus* plant microbial fuel cells for sustainable energy production

N'Gissa Attah[a, b*], Damgou Mani Kongnine[a,b], Pali Kpelou[a,b], Essowè Mouzou[a,b,c]

[a]*Département de Physique, Laboratorie sur l'Energie Solaire (LES), Université de Lomé, 01BP 1515, Togo*

[b]*Centre d'Excellence Régional pour la Maîtrise de l'Electricité (CERME), Université de Lomé, 01BP 1515, Togo*

[c]*Département de Physique, Laboratoire de Physique des Matériaux et des Composants à Semi-conducteurs, Université de Lomé, 01BP 1515, Togo*

Abstract. Plant Microbial Fuel Cells (PMFCs) are bioelectrochemical systems that harness plant rhizodeposition to generate electricity. This technology enables electrical energy to be produced while the plant grows. However, the major problem preventing the commercialization of these cells is their low power. In the present study, a systematic investigation was conducted to ascertain the optimal configuration of these cells, with the objective of determining the optimum inter-electrode distance. In the present stidy, the lemongrass plant (*Cymbopogon citratus*) was used as the main substrate source, plastic pots and graphite electrodes, while examining three single pair of electrodes configurations (PMFC-A, PMFC-B, PMFC-C), along with a unique configuration with three unaligned cathodes (PMFC-D) and three inter-electrode distances (5cm, 7.5cm and 12.5cm) were examined. The experiment focused on determining electrical parameters, plant mass growth rates and soil characteristics. These variables were measured before and after the experiment. The results indicated that the plant mass growth rate of PMFC-D exhibited the greatest magnitude (80.62%). The organic matter (OM) content in the soil exhibited an increase in each PMFC over the course of the experiment. PMFC-B exhibited the highest values of OM, electrical conductivity, and water content, respectively equal to 15.69%, 376.00µS/cm, and 15.46%. Conversely, it exhibited the lowest pH value (7.37). Electrical parameter measurements have demonstrated that PMFCs with a single pair of electrodes exhibit superior performance in comparison to those with three unaligned cathodes. Similarly, these measurements indicated that for the single pair electrode configuration, an inter-electrode distance of 7.5cm was optimal, yielding a maximum power density of 127mW/m². The determination of the average internal resistance, open circuit voltage, and power density (PD), along with their standard deviations, demonstrated that PMFC-B exhibited superior performance. Furthermore, an analysis of its autonomy revealed that the PDmin it delivers, even in the absence of sunlight, is 16.90 mW/m². From these results, PMFC-B is the best configuration for lemongrass PMFC.

Keywords: Plant Microbial Fuel Cells; electricity; configuration; inter-electrode distance; autonomy.

Received: 2nd April 2025; Revised: 16th August 2025; Accepted: 5th Sept 2025; Available online: 10th Sept 2025

1. Introduction

The accelerated processes of industrialization and urbanization have contributed to an escalated demand for energy resources worldwide, a phenomenon that has intensified significantly in the contemporary epoch defined as the Anthropocene. According to the 2022 report by the International Energy Agency (IEA, 2022), approximately 80% of the global energy mix consists of fossil fuels. These fuels are associated with the emission of greenhouse gases, which are known to contribute to climate disruption, ocean acidification, and biodiversity loss. Confronted with these challenges, the transition to renewable, sustainable, and environmentally friendly energy sources emerges as an inevitable necessity. This transition to clean energy not only helps mitigate climate change but also enhances energy security by reducing dependence on imported fossil fuels (Hoang *et al.*, 2022), thereby promoting economic resilience. Innovative technological solutions, such as Plant Microbial Fuel Cells, are being developed to address this need. These emerging technologies are poised to play a critical role by converting the biochemical energy of plants into electricity, thus offering a sustainable and environmentally-friendly alternative.

The generation of electricity by these systems relies on the natural processes of photosynthesis and rhizodeposition. Indeed, the rhizosphere microbiome plays a crucial role in the generation of electricity through the process of oxidation. This process occurs when microorganisms within the *Rhizosphere* oxidize organic compounds released by plant roots, thereby generating electrons. These electrons are subsequently transferred to an anode, and then to a cathode via an external circuit (Hasan *et al.*, 2023).

However, the energy efficiency of these innovative systems remains constrained by various factors, including soil conductivity, the selection of electrode material, the type of plant, and, most significantly, the inter-electrode distance. The latter has been shown by Schievano and colleagues to have a direct effect on the internal resistance of the system and on the proton transfer rate. As Schievano's research demonstrates in

* Corresponding author
Email: attahalexis13@gmail.com (N. Attah)

https://doi.org/10.61435/ijred.2025.61269
ISSN: 2252-4940/© 2025.The Author(s). Published by CBIORE

its study of *Spartina anglica*, this distance directly impacts two key aspects of the microbial ecosystem's functionality: the internal resistance and the proton transfer rate (Schievano, 2017). Moreover, Bataillou *et al.* demonstrated that, in systems where the inter-electrode distance is less than 7 cm, oxygen diffusion towards the anode significantly reduces the performance of their PMFC (Bataillou *et al.*, 2022). Furthermore, Takanezawa *et al.* found that in the same configuration, the 5 cm distance yielded superior performance in comparison to the 2 cm distance (Takanezawa *et al.*, 2010). Subsequent studies have examined the optimization of this distance for various plant species, including rice (Watanabe & Nishio, 2010) and swamp species (Wetser *et al.*, 2015). Additionally, Helder and his group have demonstrated that decreasing this distance enhances current density, albeit with constraints associated with ion saturation in the medium (Helder *et al.*, 2012).

The plant type is among the factors that influence the performance of PMFCs. A diverse array of plant species has been employed in PMFC, encompassing traditional wetland plants, early bioelectric plant species, hydrophytes, drought-tolerant plants, and mesophytes (Rusyn, 2021; Kabutey *et al.*, 2019; Regmi & Nitisoravut, 2020). In several instances, the advancement in bioelectricity generation was only attainable through the modification of plant species, irrespective of electrode configuration or design, and with the utilization of the same installation (Helder *et al.*, 2010; Wang *et al.*, 2017; Oodally *et al.*, 2019). These findings underscore the significance of meticulous plant species selection and the optimal configuration of electrodes in maximizing the performance of PMFCs. The best plant must demonstrate both high survival capacity in unfavorable growing conditions and a high rate of photosynthesis, accompanied by a good release rate of organic matter into the soil (Apollon *et al.*, 2021). Lemongrass (*Cymbopogon citratus*) is classified as a C4-type plant, which possesses a superior photosynthetic rate and a greater rhizodeposition of exudates into the rhizosphere compared to C3-type plants (Fernie & Bauwe, 2020). Additionally, lemongrass exhibits a high degree of adaptability, thriving in a wide range of temperature conditions, spanning from 15 to 40°C, and exhibiting tolerance to diverse soil pH levels between 4.5 and 8.5 (Kumar & Jat, 2020). This broad pH and temperatures range suggest a potential for optimal growth in PMFCs, underscoring the adaptability of lemongrass to diverse ecological conditions.

Furthermore, other researchers have explored innovative electrode configurations to maximize the contact area and minimize energy losses (Bombelli *et al.*, 2016). However, there is a paucity of research on aromatic plants such as lemongrass, whose dense root system and high exudate production could influence the optimal distance and favor electrical performance (Chong *et al.*, 2025). Moreover, the majority of studies have focused on simple configurations, often utilizing a single pair of electrodes, neglecting the vast potential of multi-electrode configurations.

This study aims to investigate two different configurations for a microbial fuel cell based on lemongrass, a plant chosen for its robustness and ability to produce root exudates rich in organic compounds. The first configuration involves a pair of electrodes with three distinct inter-electrode distances (5,0 cm, 7.5 cm, and 12.5 cm), while the second configuration involves an innovative arrangement of three unaligned cathodes, where a central anode is surrounded by three cathodes placed at different distances. The main objective of this study is to ascertain the impact of these configurations on energy production. The investigation will emphasize the optimization of the inter-electrode distance to maximize power output.

2. Materials and methods

2.1 Experimental set-up

A total of four single-chamber Plant Microbial Fuel Cells (PMFCs) have been constructed, with plastic pots serving as the fundamental container. Each pot possesses a capacity of 2.5 liters, a top diameter of 17 cm, a bottom diameter of 14 cm, and a height of 11.5 cm. Prior to utilization, the pots underwent a thorough cleaning process to ensure sterility and prevent contamination. Three of the PMFCs contain a single pair of electrodes (anode and cathode), while the fourth cell contains four electrodes, with one serving as the anode and the remaining three as the cathodes.

The graphite electrodes utilized in this study are indistinguishable, exhibiting a cylindrical shape with a diameter of 0.64 cm and a length of 5.65 cm, resulting in a surface area of 0.0012 m². The dimensions of the electrodes were measured with a precision caliper with a 0.1 mm scale. These electrodes were recovered from new Leclanché batteries. The selection of this particular type of electrode was primarily influenced by two key factors. Firstly, there is an abundance of Leclanché batteries, and presente a significant cost advantage over commercial graphite. Subsequent to the recovery process, the electrodes were meticulously cleaned using a toothbrush, rinsed with distilled water, and then placed in a ventilated room for a 48 hour drying period. Each electrode is connected to a 2.5 mm² copper wire, which functions as a current collector.

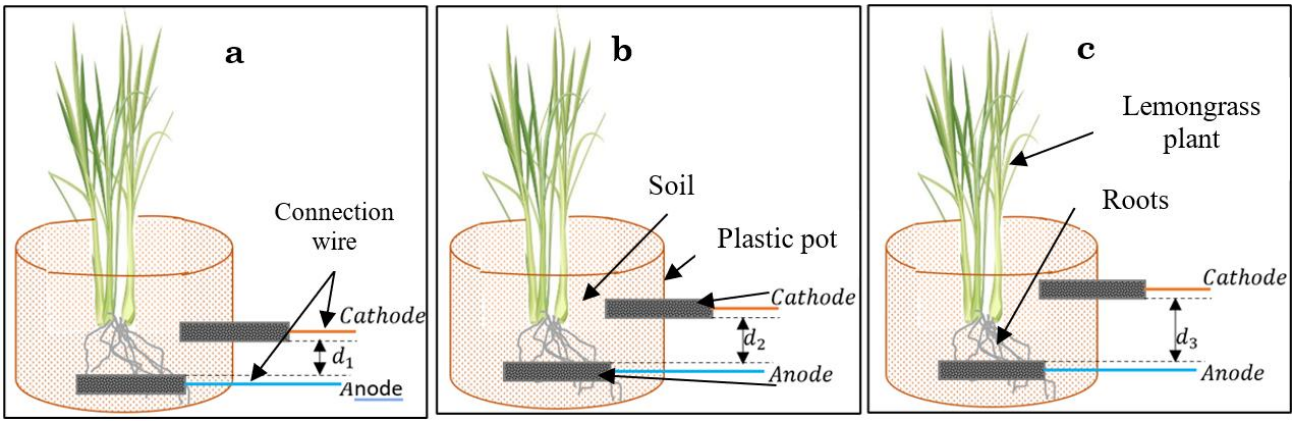

Fig. 1 Diagrams of PMFC with single pair electrodes: a) PMFC-A (5,0 cm); b) PMFC-B (7.5 cm) and c) PMFC-C (12.5 cm)

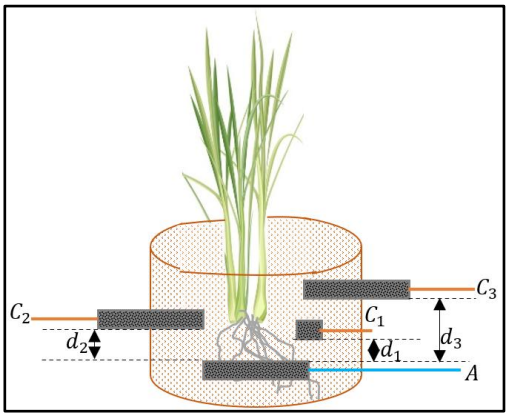

Fig. 2 Diagram of PMFC with three unaligned cathodes

Lateral holes were then drilled in each of the pots. These perforations facilitate the precise placement of the cathodes. The organic planting soil used in this study was collected in the vicinity of the LES laboratory. The lemongrass plant was utilized as the primary substrate source. The four microbial fuel cells were constructed with plants that had an equal mass of 89 g. Prior to assembly, the soil was sieved to ensure homogeneity. A total mass of 3.200 kg (±0.001 kg) of sieved soil was used to fill each pot. However, the filling process was executed in two stages: initially, 0.640 kg of soil, equivalent to one-fifth of the total mass, was added and leveled. Subsequently, the anode was positioned, and the plant was situated so that its roots covered the anode. The cathodes were then placed in the corresponding holes, ensuring that the distances between the electrodes were d1 = 5,0 cm, d2 = 7.5 cm, and d3 = 12.5 cm (Figures 1 and 2). The remaining soil (2.560 kg) was then added. These distances were selected based on prior research, which identified them as optimal values for this study. (Takanezawa *et al*., 2010; Bataillou *et al*., 2022). For the three-cathode configuration, these cathodes were placed in the pot around the anode in a non-aligned manner, also respecting the distances d1 = 5,0 cm, d2 = 7.5 cm and d3 = 12.5 cm. The three cathodes are all positioned above the anode at an angle of 120° between the axes of two consecutive cathodes. The single-electrode cells were named PMFC-A, PMFC-B and PMFC-C for the inter-electrode distances of 5,0 cm, 7.5 cm and 12.5 cm, respectively (Figure 1). The one with three unaligned cathodes was named PMFC-D (Figure 2). The numbers 1, 2, and 3 were added after the letter D during measurements to denote the cathodes at 5,0 cm (C1), 7.5 cm (C2), and 12.5 cm (C3) from the anode, respectively. Each plant was watered with 1.16 liters of tap water to create a moist environment and promote ion exchange. Once completed, the cells were placed in the sun on a one-story building slab.

2.2. Operation

The PMFCs were irrigated once a day at 6:00 p.m. with an equivalent volume of water (0.33 liters). The open-circuit voltage, on-load voltage across a 100 Ohm resistor, and the current flowing through this resistor were measured three times a day (8:30 a.m., 12:30 p.m., and 5:30 p.m.) for 35 days. The measurements were obtained using a 15XP-B multimeter. For PMFC-D, measurements were taken individually between each cathode and the anode, observing a latency time of 5 minutes between them.

To ascertain the diurnal period during which the PMFC-B's performance is at its zenith and its autonomy, measurements were taken successively at 8:30 a.m., 12:30 p.m., 5:30 p.m., 8:30 p.m., 1:30 a.m., and 8:30 a.m. of the following day from day 33 to day 34. Each of these measurements was coupled with measurements of solar irradiance, ambient temperature, and temperature inside the PMFCs using a Frederiksen 489025 pyranometer and a K-type thermocouple. Irradiance was measured at the slab bottom and at the level of the plant leaves. The temperature within PMFC was measured at three distinct points (top, middle, and bottom), subsequently averaged, and presented. At the end of the experiment, the plants were meticulously extracted, thoroughly washed with tap water, and dried in a ventilated room for a period of 12 hours. Their mass was subsequently measured, and their mass growth rates were determined.

2.3 Plant growth medium analysis

2.3.1 Sample preparation

The soil that formed the biological growth medium for the plants in our PMFCs, was analyzed at the start and end of the experiment. The final soil from each PMFC was manually mixed after the electrodes had been removed and the plant had been extracted. Then, samples were collected for analysis.

2.3.2 Water content

A precise quantity of 20 g (± 0.001 g) of soil was sampled and subsequently oven-dried at 105°C for a period of 12 hours. The water content was determined by calculating the difference between the wet and dry masses.

2.3.3 pH and electrical conductivity

20 g (± 0.001 g) of both initial and final soil from each PMFC were collected, and 100 ml of distilled water was added to each sample. The samples were then subjected to magnetic stirring for a duration of 15 minutes. Subsequently, the pH, temperature, and conductivity probes were inserted into the samples, and the values were recorded following a period of stabilization.

2.3.4 Organic matter content

Five g (± 0.001 g) of the dry soil from the moisture content determination was collected and placed in a pre-weighed porcelain crucible. The crucible was then placed in an oven at a temperature of 600°C for one hour for calcination (Kongnine *et al*., 2020). Subsequent to the calcination process, the crucible and its contents were weighed when the oven temperature decreased to 105°C. The organic matter content was determined by the difference in weight.

2.3.5 Calculations and Data Analysis

The power density was calculated using the formula:

$$P_D = \frac{V_R \times I_R}{A_{anode}} \quad (1)$$

In the above equation, V_R is the on-load voltage across the resistor, I_R is the current through the resistor, A_anode is the anode area, and P_D is the power density.

The daily average open circuit voltage and on-load voltages, the daily average current, and the daily average power density were calculated using the "mean" function in Excel. To analyze the data obtained, the evolution curves over time of the daily averages of each quantity were plotted in OriginPro 2018.

This was done to highlight the effect of the inter-electrode distance and to compare the configuration with one pair of electrodes and that with three unaligned cathodes. The internal resistance of each PMFC was first calculated using the following formula (Liu *et al*., 2008):

$$R_{in} = \frac{V_{OC} - V_R}{I_R} \quad (2)$$

In this formula, R_{in} denotes the internal resistance and V_{OC} represents the open circuit voltage. The mean of each internal resistance, $R_{in}\ av$, was subsequently determined.

Subsequently, the mean power density, the total power density produced over the 35-day period, the standard deviation of the open circuit voltage, and the daily power density of each PMFC were calculated using the "mean," "sum," and "standard deviation" formulas in Excel.

3. Results and Discussion

3.1 Soil Characteristics and Plant Growth

As illustrated in Table 1, the initial and final soil pH, water content and organic matter levels were measured, in addition to the mass growth rate of the plants utilized as the primary substrate source. The table also presents the electrical conductivity of the soil at the beginning and end of the experiment. It is clearly from the data that the pH of the growth medium, which was initially 8.04, underwent a decline for each PMFC during the course of operation. The pH level of PMFC-C was 7.96 at the end of the experiment, while PMFC-B exhibited the lowest level of 7.37. This decline in basicity in PMFCs can be attributed to the release of acidic compounds, particularly H^+ protons, during PMFC operation. The electricity produced by a PMFC originates from the oxidation of substrates, leading to the generation of electrons and protons. The organic matter (OM) content exhibited an increase at the end of the experiment, irrespective of the specific PMFC. The initial OM content was 8.00%, and it increased to 9.04%, 9.62%, 10.00%, and 15.69%, respectively, for PMFC-D, PMFC-A, PMFC-C, and PMFC-B at the conclusion of the 35-day study. This result indicates that as the plant matures, it releases an increasing amount of organic matter into the soil. The values of organic matter content are in the same order of growth as those of water content (WC) in the PMFCs, but they are in reverse order to the growth rate of the plants in the pots. PMFC-B exhibited the highest WC and OM values (15.46% and 15.69%, respectively), yet it demonstrated the lowest mass growth rate (18.54%). Conversely, PMFC-D, which exhibited the highest plant mass growth rate, demonstrated the lowest WC and OM values (9.90% and 9.04%, respectively). This suggests that PMFC-B would generate more electricity with greater autonomy than the other three PMFCs, given that its pot contains more substrate (organic matter) and a humidity more conductive to the movement of charge carriers. It is noteworthy that on the final day of measurements, the plants were not removed from the pots until 6:30 p.m., at which point photosynthesis had already ceased. Consequently, the plants initiated the process of respiration and nutrient uptake from the soil. The nutrient uptake and water requirements of the plants are proportional to their size, which could explain the low water and organic matter content of PMFC-D (Tsukagoshi & Shinohara, 2020; Marschner's Mineral Nutrition of Higher Plants, 2012). The variation in mass growth rate can be attributed, on the one hand, to the quantity or length of roots or leaves initially possessed by each lemongrass plant. Prior to potting, our primary concern was the weight of the plants. Conversely, this variation can be attributed to the influence of the electric or electromagnetic fields generated within each cell during the measurement of electrical parameters. Indeed, the presence of an electric field is a consequence of the difference in potential between the anode and cathode of each PMFC during the measurements. According to the extant literature, it has been demonstrated that artificial electric fields can exert a retarding effect on plant growth. (Pelesz & Fojcik, 2024; Rezaei-Zarchi *et al*., 2012). Indeed, the impulsive electric fields generated during each measurement, despite their low intensity (hundreds of millivolts per centimeter), can induce oxidative stress by increasing the production of free radicals, such as reactive oxygen species. These free radicals have been observed to cause damage to plant cells and tissues (Sharma *et al*, 2012). This field has also the capacity to modify ion flows within plants, thereby exerting a negative impact on growth and development. Given that the intensity of the electrostatic field is inversely proportional to the square of the distance between the electrodes, it is evident that this field decreases with distance. Consequently, the PMFC-A plant is expected to exhibit a lower mass growth rate compared to the PMFC-B plant, given that the reduced inter-electrode distance generates a high electric field intensity. This discrepancy can be rationalized by the phenomenon that, at the reduced inter-electrode distance observed in PMFC-A, the substrate would tend to diffuse towards the cathode. Consequently, the oxidation of the substrate near the cathode would result in recombination of charge carriers. This recombination would therefore cancel out part of the electrostatic field strength. The geometric configuration of the three-cathode non-aligned PMFC (PMFC-D) suggests that the resultant of the three fields generated would be weaker than that of the single-electrode PMFCs, leading to a higher mass growth rate of the plant inside. In fact, although the three cathodes are arranged at 120° to each other, perfect symmetry (equal distances) would have resulted in a zero field at the center. In our case, the symmetry is broken by the varying distances (5,0 cm, 7.5 cm, 12.5 cm). However, the field vector components do

Table 1
Initial and final soil characteristics

PMFC	At the beginning of the experiment					At the end of the experiment					
	Plant Mass (g)	pH at 29,40°C	WC (%)	OM (%)	σ (µS/cm)	Plant Mass (g)	Growth rate (%)	pH at 29.74°C	WC (%)	OM (%)	σ (µS/cm)
PMFC-A	89.00	8.04	0.76	8.00	40.20	118.40	33.03	7.50	10.79	9.62	255.00
PMFC-B	89.00	8.04	0.76	8.00	40.20	105.50	18.54	7.37	15.46	15.69	376.00
PMFC-C	89.00	8.04	0.76	8.00	40.20	117.60	32.21	7.96	10.32	10.00	180.40
PMFC-D	89.00	8.04	0.76	8.00	40.20	160.75	80.62	7.68	9.90	9.04	272.00

not add up constructively. The 120° angles and variations in distance result in the partial cancellation of the components, thereby reducing the result. As previously indicated, the intensity of the field decreases in proportion to the square of the distance. Consequently, the cathode that is closest to the anode (5,0 cm) exerts a greater influence on the total field than the other cathodes. However, the contributions of the more distant cathodes (particularly at 12.5 cm) are small, and their directions (at 120° and 240°) partially oppose that of the nearby cathode, which reduces the result. Furthermore, an increase in electrical conductivity of the substrate was observed over the course of the experiment at the level of each PMFC, which indicates an increase in the number of charge carriers released during the operation of these PMFCs. This increase in charge carriers can be attributed to the proliferation of bacteria that oxidize the substrate. The PMFC that exhibited the highest conductivity value was PMFC-B, which registered at 376.00 µS/cm, suggesting a high concentration of ionic conductors within this particular PMFC.

3.2 Maximum and minimum electrical values

The maximum and minimum values of open circuit voltage and power density produced by PMFCs with one pair of electrodes and three unaligned cathodes are given in Tables 2 and 3, respectively. As shown in Table 2, for single pair electrode PMFCs, the maximum open circuit voltage values are 702 mV, 558 mV, and 448 mV obtained with PMFC-B at 8:30 am on day 29, PMFC-A at 12:30 am on day 6, and PMFC-C at 8:30 am on day 6, respectively. It is noteworthy that PMFC-A and PMFC-C exhibited equivalent minimum open circuit voltage values (79 mV), while PMFC-B demonstrated a 2.6-fold higher minimum value (208 mV).

The maximum power density of the single pair electrode PMFCs followed a similar trend as the open circuit voltage. The highest power density value of 127 mW/m^2 was obtained on day 29 with PMFC-B. This value is 7.06 times higher than that obtained by Aziri et al. (Azri *et al*., 2018), who also used graphite electrodes and the same external resistance value. In a similar vein, Widharyanti and colleagues reported a value that was 1.27 times lower than our own (Widharyanti *et al*., 2021). On the 29th day, the PMFC exhibited a maximum current intensity of 1.20 mA, in contrast to the 0.92 mA recorded by Bataillou and his team (Bataillou *et al*., 2022) at the same inter-electrode distance. This outcome serves to demonstrate three things. Firstly, it demonstrates the performance of the lemongrass plant. Secondly, it demonstrates the optimized inter-electrode distance that was used in the present study. And thirdly, it demonstrates the effectiveness of the methodology that was employed. The power densities of PMFC-A and PMFC-C were recorded as 80.85 mW/m^2 on day 11 and 26.10 mW/m^2 on day 16, respectively. The lowest recorded power density value (0.05 mW/m^2) was obtained with PMFC-C on day 31.

In the case of the PMFC with three unaligned cathodes (PMFC-D), 5,0 cm inter-electrode distance (PMFC-D1) demonstrated the maximum power density (41.68 mW/m^2, obtained on day 6, signifying its efficacy in this configuration. With regard to open circuit voltage, 7.5 cm (PMFC-D2) and 12.5 cm (PMFC-D3) exhibited similar values of 545 mV and 543 mV, respectively. These values are significantly lower than those observed in single pair electrode PMFCs.

Table 2
Maximum and minimum values for open-circuit and on-load voltages, current intensity and power density of single pair electrodes PMFCs

Parameters	PMFC-A			PMFC-B			PMFC-C		
	Value	Day	Moment	Value	Day	Moment	Value	Day	Moment
V_{OCmax} (mV)	558	6th	12 :30	702	29th	8 :30 am	448	6th	8 :30 am
V_{OCmin} (mV)	79	31st	5 :30 pm	208	32th	12 :30	79	32th	12 :30
V_{Rmax} (mV)	99	11th	8 :30 am	124	29th	8 :30 am	82	25th	8 :30 am
V_{Rmin} (mV)	3	31st	5 :30 pm	6	33th	5 :30 pm	3	31th	5 :30 pm
I_{Rmax} (mA)	0.98	11th	8 :30 am	1.20	29th	8 :30 am	0.56	20th	12 :30
I_{Rmin} (mA)	0.02	30th	8 :30 am	0.06	3rd	5 :30 pm	0.02	31st	5 :30 pm
P_{Dmax} (mW/m^2)	80.85	11th	8 :30 am	127	29th	8 :30 am	26.10	16th	8 :30 am
P_{Dmin} (mW/m^2)	0.08	33rd	5 :30 pm	0.30	3rd	5 :30 pm	0.05	31st	12 :30

Table 3
Maximum and minimum values for open-circuit and on-load voltages, current intensity and power density of three non-aligned cathodes PMFC

Parameters	PMFC − D1			PMFC − D2			PMFC − D3		
	Value	Day	Moment	Value	Day	Moment	Value	Day	Moment
V_{OCmax} (mV)	524	5th	8 :30 am	545	7th	8 :30 am	543	5th	8 :30 am
V_{OCmin} (mV)	45	28th	5 :30 pm	40	27th	8 :30 am	25	27th	5 :30 pm
V_{Rmax} (mV)	94	5th	8 :30 am	78	8th	8 :30 am	74	21st	8 :30 am
V_{Rmin} (mV)	2	28th	5 :30 pm	2	34th	12 :30	2	2nd	8 :30 am
I_{Rmax} (mA)	0.67	14th	8 :30 am	0.63	6th	8 :30 am	0.69	19th	8 :30 am
I_{Rmin} (mA)	0.02	28th	5 :30 pm	0.01	34th	12 :30	0.01	3rd	8 :30 am
P_{Dmax} (mW/m^2)	41.68	6th	8 :30 am	39.38	6th	8 :30 am	36.38	21st	8 :30 am
P_{Dmin} (mW/m^2)	0.03	28th	5 :30 pm	0.02	34th	12 :30	0.03	3rd	8 :30 am

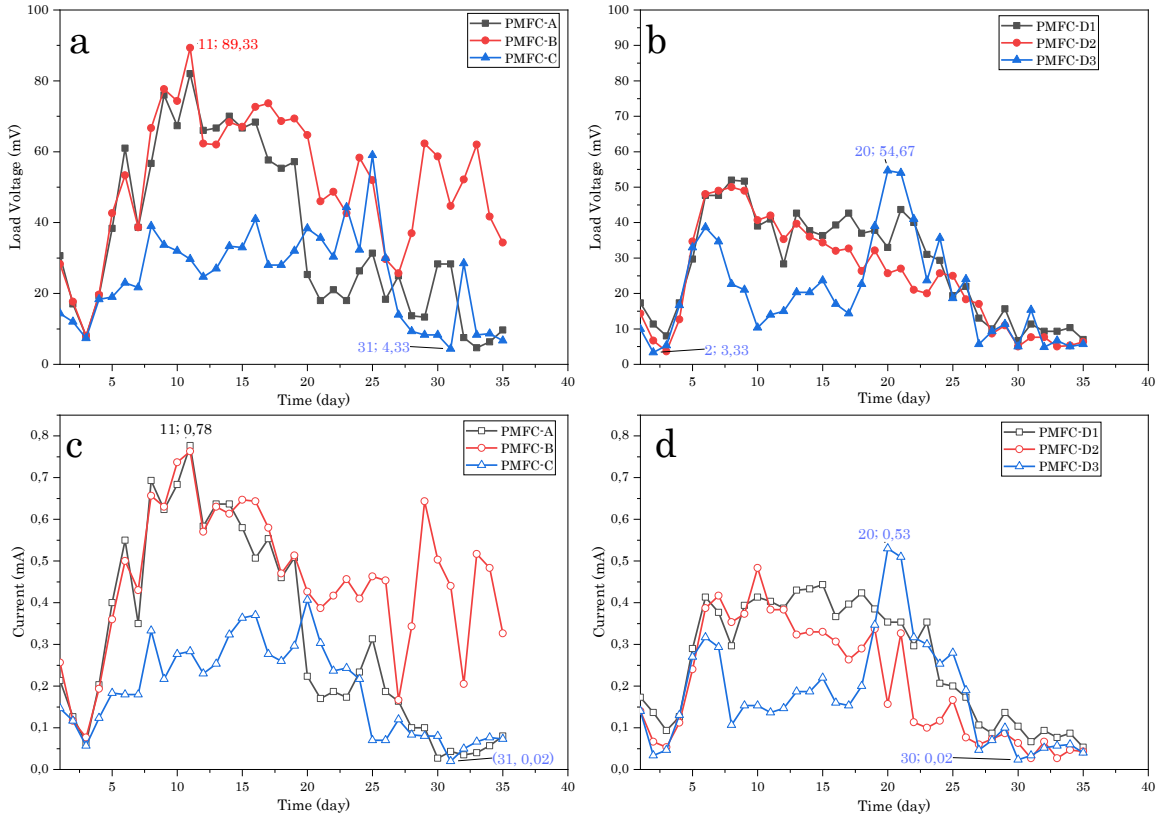

Fig. 3 Load voltages and currents: a) and c) Single pair electrode configuration; b) and d) Three unaligned cathodes configuration

3.3 Load voltages and currents

As demonstrated in Figure 3, the mean daily charge voltage and current for the various PMFCs exhibit a consistent trend. Irrespective of configuration type and electrode distance, charging voltages and intensities manifest nearly identical trends, comprising four phases: a decrease phase, a growth phase, a stabilization phase, and a decrease phase. During the initial 3 days, minimal activity is observed, which may be attributed to the necessary time for the formation of the electroactive biofilm on the anode and the production of enzymes required for electron transfer from the bacterial cell (Conners *et al.*, 2022). Concurrently, the lemongrass plant adapts to its novel environment during this phase. Subsequent to the initial 3-day period, a marked increase in voltage and intensity is observed, reaching 89.33 mV for PMFC-B and 0.78 mA for PMFC-A, respectively. This phenomenon can be attributed to the formation of a biofilm on the anode surface through substantial proliferation of microorganisms. (Widharyanti *et al.*, 2021). From day 8 to day 20, these electrical values remain relatively stable. The negligible fluctuations observed are hypothesized to be attributable to the intermittent substrate production by the citronella during photosynthesis, resulting from the absence of continuous solar irradiation. Subsequent to 20 days of activity, voltages and intensities undergo a progressive decline, likely attributable to a series of limiting reactions imposed by the specific bacterial communities catalyzing the anodic reaction, which reduce the overall potential difference (B. E. Logan, 2007), or alternatively, to a change in the composition of the microbial community influenced by time and several factors such as physico-chemical variations in the soil (pH, temperature, and carbon, nitrogen, and phosphorus content, etc.). In addition to the previously mentioned factors, plant-microorganism interactions (Lozano *et al.*, 2014) and substrate diffusion towards the cathode following plant root development would also have contributed. Furthermore, oxidation of the connecting wires at the electrode-wire contacts was also a limiting factor. The observed decline in voltage and current can also be attributed to a decrease in internal humidity within the PMFCs, which has a deleterious effect on ionic conduction. As plants grow, they absorb more and more water. However, in this study, the amount of water used for watering was kept constant at 0.33 liters per day. As plants undergo growth, they exhibit an increased rate of water absorption. However, in this study, the amount of water used for watering was kept constant at 0.33 liters per day. As the plants undergo growth, the PMFCs undergo a gradual desiccation, leading to a reduction in their overall performance.

3.4 Open-circuit voltages and power densities

The daily averages of the open circuit voltage (OCV) and power density of the different PMFCs are shown in Figure 4. As depicted in Fig. 4a, the open circuit voltages of the single pair electrode PMFCs exhibit an increase from day 2 up to their maximum values. For the initial 15 days, the OCV values exhibited an inverse relationship with the inter-electrode distance. The smallest distance (5,0 cm) exhibited the highest value. This phenomenon could be attributed to the internal resistance, which has been observed to increase initially with inter-electrode distance (Madondo et al., 2023), or to the rapid development of biofilm on the anode (Saadi et al., 2020). Indeed, Simeon et al (Simeon & Freitag, 2022) found that wider electrode spacing delayed biofilm attachment. After the 15th day, the trend reverses and the voltage corresponding to the 7.5 cm distance takes over, while that of the 5,0 cm distance becomes the lowest. At short distances, electrodes may

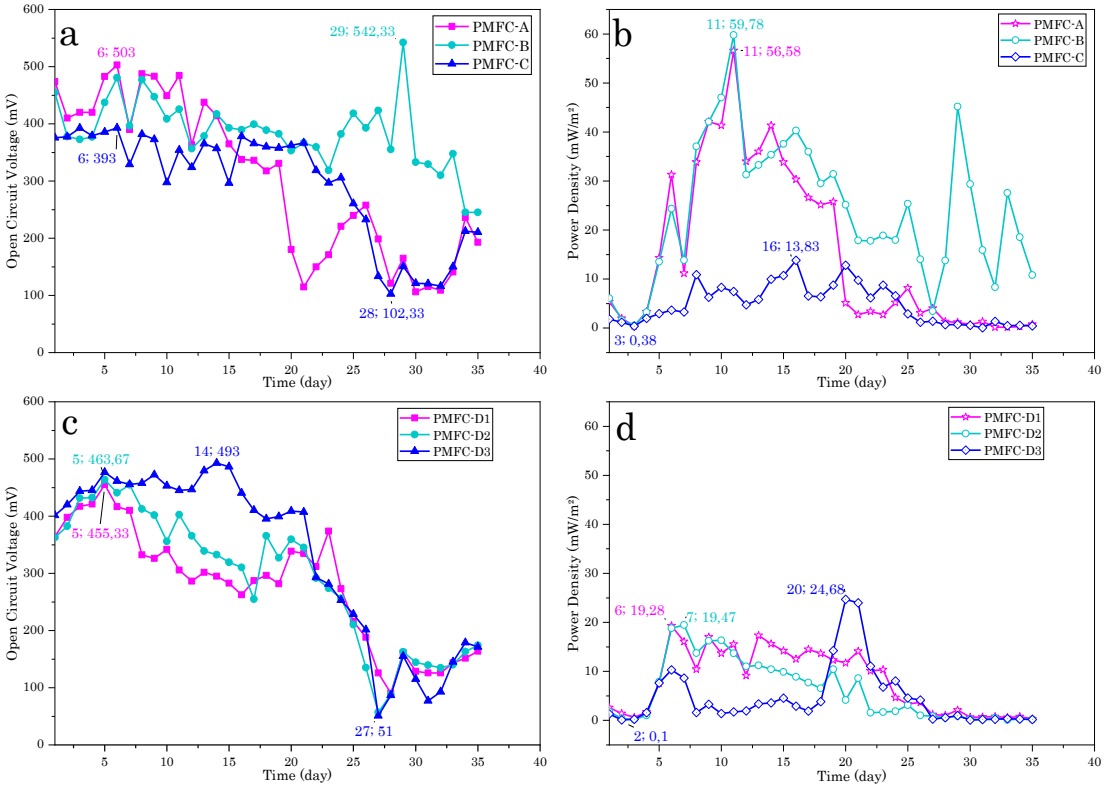

Fig. 4 Open Circuit Voltage and Power Density: a) and b) Single pair electrode configuration; c) and d) Three unaligned cathodes configuration

experience accelerated clogging due to the accumulation of reaction products or biofilms, thereby reducing their efficiency (Helder *et al.*, 2012). This phenomenon can be attributed to fouling on the electrode, which is caused by a higher concentration of substrate at the cathode electrode or by a sharp increase in biofilm thickness at the anode section (Simeon *et al.*, 2020). The maximum values of the daily average OCV of one pair electrode PMFCs with distances of 5,0 cm, 7.5 cm, and 12.5 cm are 393 mV, 542.33 mV, and 503 mV, respectively. The 7.5 cm distance appears to offer an optimal balance between reducing internal resistance and ensuring long-term nutrient availability. This distance facilitates the efficient diffusion of ions without rapidly depleting local resources.

As illustrated in Figure 4b, PMFC-B (7.5 cm) exhibited the highest power density, measuring 59.78 mW/m², followed by PMFC-A (5,0 cm) at 56.58 mW/m² and PMFC-C (12.5 cm) at 13.83 mW/m². For the PMFC with three unaligned cathodes, the evolution of the open-circuit voltage is initially a function of the inter-electrode distance (Figure 4c). During the initial 22-day period, these voltages exhibit a direct proportionality to the inter-electrode distance. The cathode positioned at 5,0 cm yields the lowest voltage (maximum value 455.33 mV), while the cathode at 12.5 cm generates the highest voltage (maximum value 493 mV). This phenomenon can be attributed to the effect of the electrostatic field. The asymmetrical arrangement of the cathodes around the anode gives rise to a non-uniform electrostatic field. Ions generated by the plant's metabolic activity, particularly by substrate oxidation, migrate towards the cathodes. However, their distribution is influenced by the distance and geometry of the system (Bard & Mirkin, 2001). The furthest cathode may be situated in a region of higher electric field intensity due to spatial configuration and ion accumulation, which explains the reversal of observations compared to single pair electrode PMFCs. In this configuration, the inter-electrode distance exerts a predominant influence on performance, a consequence of both internal resistance and constrained ion diffusion. After day 22, the curves illustrating these tensions diminish but remain intertwined. These observations can be attributed to the varying oxidation states of the conductive wires utilized as electron collectors at the electrode-wire interfaces, or to the gradual decline in humidity within the PMFC as the plant undergoes growth.

The power density of the PMFC with three unaligned cathodes exhibited a maximum at a distance of 12.5 cm (24.68 mW/m²). This value is more than 2.4 times lower than that recorded for PMFC-B. However, the temporal evolution of the power density reveals that this maximum is an isolated value. Specifically, the power density at the 12.5 cm distance was lower during the initial 19 days and from day 26 onwards (Figure 4d). The power density of 5,0 cm (PMFC-D1) appears to increase over time. This observation will be further elucidated in the subsequent paragraph, which presents the mean and total values produced.

These results demonstrate that the performance of a PMFC is significantly influenced by the spatial configuration of electrodes and the temporal evolution of electrochemical conditions. During the initial phase, the inter-electrode distance emerges as the predominant factor, aligning with the tenets of electrochemistry. However, as ions accumulate and the electrostatic field is modified, this relationship is reversed, underscoring the significance of electrostatic interactions in intricate bioelectrochemical systems such as Plant Microbial Fuel Cells.

Table 4
Comparaison and advantages of single pair configurations over three unaligned configuration

PMFC	PMFC − A	PMFC − B	PMFC − C	PMFC − D1	PMFC − D2	PMFC − D3
$P_{D\ avarage}$ (mW/m^2)	15.29	24.11	4.84	8.03	6.04	4.59
$P_{D\ tot}$ (mW/m^2)	535.32	843.87	169.44	281.20	211.57	160.50
Standard deviation of V_{OC}	136.33	59.27	97.44	102.68	117.46	147.37
$R_{in\ av}$ (Ω)	1 435.50	1 101.74	2 116.47	1 420.68	2 658.90	3 492.85

3.5 Comparative study of configurations

In the single pair electrode configuration, the inter-electrode distance exerts a pivotal influence on the performance of the PMFC. A comparative study of the different configurations was carried out (Table 4) based on the average and total power densities produced by the PMFCs and the standard deviation of their open-circuit voltages over the 35 days of measurements. The results indicate that for single pair electrode PMFCs, the 7.5 cm distance yielded the highest mean and total power (24.11 mW/m² and 843.87 mW/m², respectively), while the 12.5 cm distance yielded the lowest values (4.84 mW/m² and 169.44 mW/m², respectively). The 5,0 cm distance exhibited intermediate values (15.29 mW/m² and 535.32 mW/m²). Consequently, the 7.5 cm distance is indicative of an optimal equilibrium between internal resistance and ion availability within the medium. A short distance (5,0 cm) can result in ion saturation around the electrodes, which can limit diffusion and increase polarization losses. Conversely, an increased distance (12.5 cm) has been shown to enhance internal resistance due to the augmented ion path length, thereby reducing PMFC efficiency (2,116.47 Ω for the 12.5 cm distance vs. 1,101.74 Ω for 7.5 cm). These phenomena elucidate the existence of an optimal zone for electrochemical activity within single pair electrode PMFCs. This zone is characterized by a sufficient concentration of organic substrates to feed the micro-organisms, minimal internal resistance to facilitate electron transfer, and a balance between proton production and consumption to maintain a favorable pH (7.37) and a better electrical conductivity of the medium (376.00 µS/cm). In the case of lemongrass, this zone is approximately 7.5 cm. Zingbe et al. (2025) recently found that 5 cm was the optimum distance using the same plant (Zingbe *et al*., 2025). This discrepancy could be attributed to the difference in the number of study days, which was limited to 18 in their study and 35 in the present study. As demonstrated in the present study and numerous others (Madondo *et al*., 2023; Simeon *et al*., 2020), an initial increase in internal resistance is observed with increasing inter-electrode distance. However, after approximately two weeks of operation, this trend undergoes a reversal. This reversal is attributed to the development of plant roots, the diffusion of substrate, and the increase in thickness of the biofilm.

The unaligned three-cathode PMFC introduces a complex geometry, where a central anode is surrounded by three cathodes arranged at varying distances. In contrast to the single-electrode configuration, this PMFC demonstrates that the 5,0 cm distance yields the highest average and total power (8.03 mW/m² and 281.20 mW/m², respectively). This outcome may be attributed to the mitigation of charge losses caused by the non-aligned arrangement of the cathodes around the anode, thereby enabling a more uniform distribution of the electric current. At 5,0 cm, the proximity of the electrodes reduces charge losses and improves electron transfer, coupled with a lower internal resistance (1,420 Ω). This configuration also enables more efficient use of the organic substrate, as the electroactive microorganisms are more evenly distributed around the anode. Conversely, at greater distances (7.5 cm and 12.5 cm), the competition between cathodes to capture protons can result in energy dissipation. At 5,0 cm, this competition is minimized, thereby explaining the superior performance at this distance.

A comparison between the two configurations reveals that, irrespective of the inter-electrode distance, the average and total power densities generated by the one-electrode-pair PMFCs are notably higher than those produced by the unaligned three-cathode PMFC. The determination of the standard deviation of the open-circuit voltage reveals that the 7.5 cm distance yields the lowest value (59.27) for the one-electrode-pair configuration. This finding indicates that the 7.5 cm distance optimizes the electrochemical interactions between the electrodes, thereby facilitating more stable electricity generation. In contrast, the three-cathode, non-aligned configuration exhibited the lowest standard deviation value at a distance of 5,0 cm. This finding underscores the pivotal role that inter-electrode distance and PMFC configuration play in ensuring the stability of open circuit voltage. A distance of 7.5 cm appears to be an optimal compromise for the single-electrode-pair PMFCs, while the unaligned three-cathode configuration benefits from a shorter distance (5,0 cm) to maximize stability.

In the case of a lemongrass PMFC, the configuration with a pair of electrodes 7.5 cm apart offers the best performance in terms of voltage, power density, and electrical stability. However, the selection of a particular configuration is contingent upon the intended application of the PMFC. The configuration with three unaligned cathodes presents a promising alternative for applications necessitating the concurrent utilization of multiple low-power receivers.

3.6 PMFC-B autonomy

One of the most salient parameters of a battery is its autonomy. Autonomy is defined as the duration for which a battery can supply energy before requiring recharging. In the context of a Plant Microbial Fuel Cell, this term signifies the system's capacity to generate energy in a continuous and autonomous manner, without necessitating external intervention for its operation. The autonomy of the PMFC with a pair of electrodes 7.5 cm apart was investigated over a 24-hour period, from 8:30 a.m. to 8:30 a.m. the following day, by analyzing the evolution of power density as a function of internal temperature and solar irradiance. The results of this study are presented in Table 5. The findings of this study indicate a correlation between power density, temperature, and solar irradiance, with power density

Table 5
Influence of environmental parameters and PMFC – B autonomy

Parameters	8: 30 am	12: 30	5: 30 pm	8: 30 pm	1: 30 am	5: 30 am	8 : 30 am
Tam (°C)	31.70	32.40	28.30	26.80	27.40	27.70	31.68
Tin (°C)	32.47	33.43	28.53	26.93	26.83	27.03	32.50
$V_{OC\ avarage}$ (mV)	317	401	325	278	297	325	320
$P_{D\ av}$ (mW/m^2)	38.18	29.99	14.57	35.80	16.90	27.22	38.02
Ir leaves (W/m^2)	53	900	458	0	0	0	55
Ir slab floor (W/m^2)	50	894	465	0	0	0	52

peaks observed at 8:30 am and 8:30 pm. The performance of the PMFC was also influenced by watering it with lukewarm water after 5:30 pm. A peak in power density (38.18 mW/m²) was observed at 8:30 am, coinciding with moderate irradiance and optimal temperature (32.47°C). This temperature is conducive to photosynthesis and bacterial activity. Despite the presence of maximum irradiance (900 W/m²), a 21.5% decline in power density was observed at 12:30. This decline could be attributed to thermal stress, with temperatures exceeding 33°C leading to the inhibition of microbial enzymes (Hartman et al., 2019; Jiang et al., 2024). Subsequent to the irrigation, the power density exhibited an ascent to 35.80 mW/m² at 8:30 p.m., thereby substantiating the favorable influence of humidity on ionic conductivity (Helder *et al*., 2013). The incorporation of water led to a transient increase in substrate humidity, thereby facilitating both electronic and ionic transfer. However, the subsequent nocturnal decline (16.90 mW/m² at 1:30 a.m.) signifies a constraint imposed by the availability of organic substrates. Consequently, in the absence of sunlight (photosynthesis), PMFC-B exhibits a minimum power density of 16.90 mW/m² and an open-circuit voltage of 278 mV.

The lemongrass PMFC, equipped with a pair of 7.5 cm distance electrodes, exhibits promising autonomy, with production peaking during the morning and nighttime hours. Optimization of this PMFC necessitates thermal regulation within the range of 32.47°C to 32.50°C, targeted water management, and exposure to moderate irradiance.

4. Conclusion

This study examined the impact of the inter-electrode distance and configuration of a PMFC using lemongrass (*Cymbopogon citratus*) on its energy performance. The initial configuration involved a pair of electrodes with three distinct inter-electrode distances. The subsequent configuration entailed an innovative setup with three unaligned cathodes, where a central anode is encircled by three cathodes positioned at varying distances.

The results indicated that the optimum distance varies according to the configuration: 7.5 cm for the configuration with one pair of electrodes and 5 cm for the configuration with three unaligned cathodes. The calculation of the standard deviation indicated that the open-circuit voltage exhibited enhanced stability for the optimal inter-electrode distances within each configuration. However, the unaligned three-cathode configuration demonstrated suboptimal performance in comparison to the single-electrode-pair configuration. The study of PMFC autonomy with a pair of electrodes 7.5 cm apart demonstrated a correlation between power density, temperature, and solar irradiance. Furthermore, it has been demonstrated that this PMFC possesses the capacity to generate electricity in an uninterrupted manner, even in the absence of irradiance, i.e., during nocturnal periods. However, enhancing its performance necessitates thermal regulation, precise water management, and moderate irradiance exposure. Further studies are also needed to investigate the efficiency of combining cathodes in the multi-cathode configuration.

5. Future Work

In light of the results obtained, prospects for future work are emerging. In order to gain a more profound understanding of the phenomena observed during this work, it is beneficial to:
Undertake a thorough examination of the repercussions engendered by the combination of cathodes on the efficacy of the multi-cathode PMFC. Ensure that the relative humidity remains constant within the plant material growth chambers (PMFCs) through the implementation of an automated watering system that is calibrated to the dimensions of the plant or to environmental requirements. In addition, an investigation will be conducted into the aligned arrangement of cathodes in the multiple cathode configuration.

Acknowledgments

The authors gratefully acknowledge the support of all the staff of CERME and LES (Solar Energy Laboratory) for their assistance.

Author Contributions: N'Gissa ATTAH: Conceptualization, experimental manipulations, data management, formal analysis, writing - original version, Damgou MANI KONGNINE: Project management, methodology, general supervision and validation, Essowè MOUZOU: Methodology, experimental supervision, writing - revision and Pali KPELOU: Methodology, experimental supervision, writing - revision.

Funding: The work was supported by funding from the World Bank for the project "Centre d'Excellence Régional pour la Maîtrise de l'Electricité (CERME)" of Universty of Lomé (Crédit IDA 6512-TG; Don IDA 536IDA).

Conflicts of Interest: The authors declare no conflict of interest.

References

Apollon, W., Luna-Maldonado, A. I., Kamaraj, S.-K., Vidales-Contreras, J. A., Rodríguez-Fuentes, H., Gómez-Leyva, J. F., & Aranda-Ruíz, J. (2021). Progress and recent trends in photosynthetic assisted microbial fuel cells: A review. *Biomass and Bioenergy*, 148, 106028. https://doi.org/10.1016/j.biombioe.2021.106028

Azri, Y. M., Tou, I., Sadi, M., & Benhabyles, L. (2018). Bioelectricity generation from three ornamental plants: Chlorophytum comosum, Chasmanthe floribunda and Papyrus diffusus. *International Journal of Green Energy,* 15(4), 254–263. https://doi.org/10.1080/15435075.2018.1432487

Bard, A. J., & Mirkin, M. V. (Eds.). (2001). Scanning Electrochemical Microscopy (0 ed.). CRC Press. https://doi.org/10.1201/9780203910771

Bataillou, G., Haddour, N., & Vollaire, C. (2022). Bioelectricity production of PMFC using Lobelia Queen Cardinalis in individual and shared soil configurations. *E3S Web of Conferences*, 334, 08001. https://doi.org/10.1051/e3sconf/202233408001

Birol, D. F. (2022). International Energy Agency. World Energy Outlook 2022. www.iea.org

Bombelli, P., Dennis, R. J., Felder, F., Cooper, M. B., Madras Rajaraman Iyer, D., Royles, J., Harrison, S. T., Smith, A. G., Harrison, C. J., & Howe, C. J. (2016). Electrical output of bryophyte microbial fuel cell systems is sufficient to power a radio or an environmental sensor. *Royal Society open science*. https://doi.org/10.17863/CAM.6429

Chong, P. L., Chuah, J. H., Chow, C.-O., & Ng, P. K. (2025). Plant microbial fuel cells: A comprehensive review of influential factors, innovative configurations, diverse applications, persistent challenges, and promising prospects. *International Journal of Green Energy,* 22(3), 599–648. https://doi.org/10.1080/15435075.2024.2421325

Conners, E. M., Rengasamy, K., & Bose, A. (2022). Electroactive biofilms : How microbial electron transfer enables bioelectrochemical applications. *Journal of Industrial Microbiology and Biotechnology,* 49(4), kuac012. https://doi.org/10.1093/jimb/kuac012

Fernie, A. R., & Bauwe, H. (2020). Wasteful, essential, evolutionary stepping stone? The multiple personalities of the photorespiratory pathway. The Plant Journal, 102(4), 666–677. https://doi.org/10.1111/tpj.14669

Hartman, L. M., Van Oppen, M. J. H., & Blackall, L. L. (2019). The Effect of Thermal Stress on the Bacterial Microbiome of Exaiptasia diaphana. *Microorganisms,* 8(1), 20. https://doi.org/10.3390/microorganisms8010020

Hasan, Mohd. R., Anzar, N., Sharma, P., Malode, S. J., Shetti, N. P., Narang, J., & Kakarla, R. R. (2023). Converting biowaste into sustainable bioenergy through various processes. *Bioresource Technology Reports,* 23, 101542. https://doi.org/10.1016/j.biteb.2023.101542

Helder, M., Chen, W., Van Der Harst, E. J. M., & Strik, D. P. B. T. B. (2013). Electricity production with living plants on a green roof: Environmental performance of the plant-microbial fuel cell. *Biofuels, Bioproducts and Biorefining,* 7(1), 52–64. https://doi.org/10.1002/bbb.1373

Helder, M., Strik, D. P. B. T. B., Hamelers, H. V. M., Kuhn, A. J., Blok, C., & Buisman, C. J. N. (2010). Concurrent bio-electricity and biomass production in three Plant-Microbial Fuel Cells using Spartina anglica, Arundinella anomala and Arundo donax. *Bioresource Technology*, 101(10), 3541–3547. https://doi.org/10.1016/j.biortech.2009.12.124

Helder, M., Strik, D. P. B. T. B., Hamelers, H. V. M., Kuijken, R. C. P., & Buisman, C. J. N. (2012). New plant-growth medium for increased power output of the Plant-Microbial Fuel Cell. *Bioresource Technology,* 104, 417–423. https://doi.org/10.1016/j.biortech.2011.11.005

Helder, M., Strik, D. P., Hamelers, H. V., & Buisman, C. J. (2012). The flat-plate plant-microbial fuel cell: The effect of a new design on internal resistances. *Biotechnology for Biofuels,* 5(1), 70. https://doi.org/10.1186/1754-6834-5-70

Hoang, A. T., Varbanov, P. S., Nižetić, S., Sirohi, R., Pandey, A., Luque, R., Ng, K. H., & Pham, V. V. (2022). Perspective review on Municipal Solid Waste-to-energy route: Characteristics, management strategy, and role in circular economy. *Journal of Cleaner Production,* 359, 131897. https://doi.org/10.1016/j.jclepro.2022.131897

Jiang, H., Liu, J., Huang, Q., & Yang, D. (2024). Effects of Short-Term Temperature Stress on Metabolic and Digestive Enzymes Activities of Procambarus clarkii. *Israeli Journal of Aquaculture - Bamidgeh*, 76(4). https://doi.org/10.46989/001c.126179

Kabutey, F. T., Zhao, Q., Wei, L., Ding, J., Antwi, P., Quashie, F. K., & Wang, W. (2019). An overview of plant microbial fuel cells (PMFCs): Configurations and applications. *Renewable and Sustainable Energy Reviews,* 110, 402–414. https://doi.org/10.1016/j.rser.2019.05.016

Kongnine, D. M., Kpelou, P., Attah, N., Kombate, S., Mouzou, E., Djeteli, G., & Napo, K. (2020). Energy Resource of Charcoals Derived from Some Tropical Fruits Nuts Shells. *International Journal of Renewable Energy Development,* 9(1), 29–35. https://doi.org/10.14710/ijred.9.1.29-35

Kumar, M., & Jat, R. K. (2020). Lemongrass: A Valuable Crop for Soil Erosion Management. 2(11). *Agriculture & Food: E-Newsletter*. https://doi.org/10.1016/B978-0-12-816691-8.00014-5

Liu, H., Cheng, S., Huang, L., & Logan, B. E. (2008). Scale-up of membrane-free single-chamber microbial fuel cells. *Journal of Power Sources,* 179(1), 274–279. https://doi.org/10.1016/j.jpowsour.2007.12.120

Logan, B. E. (2007). Microbial Fuel Cells (1st ed.). Wiley. https://doi.org/10.1002/9780470258590

Lozano, Y. M., Hortal, S., Armas, C., & Pugnaire, F. I. (2014). Interactions among soil, plants, and microorganisms drive secondary succession in a dry environment. *Soil Biology and Biochemistry*, 78, 298–306. https://doi.org/10.1016/j.soilbio.2014.08.007

Madondo, N. I., Rathilal, S., Bakare, B. F., & Tetteh, E. K. (2023). Effect of Electrode Spacing on the Performance of a Membrane-Less Microbial Fuel Cell with Magnetite as an Additive. *Molecules*, 28(6), 2853. https://doi.org/10.3390/molecules28062853

Marschner's Mineral Nutrition of Higher Plants. (2012). Elsevier. https://doi.org/10.1016/C2009-0-63043-9

Oodally, A., Gulamhussein, M., & Randall, D. G. (2019). Investigating the performance of constructed wetland microbial fuel cells using three indigenous South African wetland plants. *Journal of Water Process Engineering,* 32, 100930. https://doi.org/10.1016/j.jwpe.2019.100930

Pelesz, A., & Fojcik, M. (2024). Effect of high static electric field on germination and early stage of growth of Avena sativa and Raphanus sativus. *Journal of Electrostatics*, 130, 103939. https://doi.org/10.1016/j.elstat.2024.103939

Regmi, R., & Nitisoravut, R. (2020). AZOLLA ENHANCES ELECTRICITY GENERATION OF PADDY MICROBIAL FUEL CELL. *ASEAN Engineering Journal*, 10(1), 55–63. https://doi.org/10.11113/aej.v10.15539

Rezaei-Zarchi, S., Imani, S., Mehrjerdi, H. A., & Mohebbifar, M. R. (2012). The Effect of Electric Field on the Germination and Growth of Medicago Sativa Planet, as a native Iranian alfalfa seed. *Acta Agriculturae Serbica*.

Rusyn, I. (2021). Role of microbial community and plant species in performance of plant microbial fuel cells. *Renewable and Sustainable Energy Reviews*, 152, 111697. https://doi.org/10.1016/j.rser.2021.111697

Saadi, M., Pézard, J., Haddour, N., Erouel, M., Vogel, T. M., & Khirouni, K. (2020). Stainless steel coated with carbon nanofiber/PDMS composite as anodes in microbial fuel cells. *Materials Research Express*, 7(2), 025504. https://doi.org/10.1088/2053-1591/ab6c99

Schievano, A. (2017). Floating microbial fuel cells as energy harvesters for signal transmission from natural water bodies. *Journal of Power* Sources.

Sharma, P., Jha, A. B., Dubey, R. S., & Pessarakli, M. (2012). Reactive Oxygen Species, Oxidative Damage, and Antioxidative Defense Mechanism in Plants under Stressful Conditions. *Journal of Botany,* 2012, 1-26. https://doi.org/10.1155/2012/217037

Simeon, M.I., Imoize, A. L., & Freitag, R. (2020). Evaluation of the electrical performance of a soil-type microbial fuel cell treated with a substrate at different electrode spacings. *Proceedings of ICEESEN2020.*

Simeon, M. I., & Freitag, R. (2022). Influence of electrode spacing and fed-batch operation on the maximum performance trend of a soil microbial fuel cell. *International Journal of Hydrogen Energy, 47(24), 12304–12316.* https://doi.org/10.1016/j.ijhydene.2021.11.110

Takanezawa, K., Nishio, K., Kato, S., Hashimoto, K., & Watanabe, K. (2010). Factors Affecting Electric Output from Rice-Paddy Microbial Fuel Cells. *Bioscience, Biotechnology, and Biochemistry,* 74(6), 1271–1273. https://doi.org/10.1271/bbb.90852

Tsukagoshi, S., & Shinohara, Y. (2020). Nutrition and nutrient uptake in soilless culture systems. In Plant Factory (p. 221-229). Elsevier.

Wang, J., Song, X., Wang, Y., Bai, J., Li, M., Dong, G., Lin, F., Lv, Y., & Yan, D. (2017). Bioenergy generation and rhizodegradation as affected by microbial community distribution in a coupled constructed wetland-microbial fuel cell system associated with three macrophytes. *Science of The Total Environment,* 607–608, 53–62. https://doi.org/10.1016/j.scitotenv.2017.06.243

Watanabe, K., & Nishio, K. (2010). Electric Power from Rice Paddy Fields. In A. Ng (Ed.), Paths to Sustainable Energy. InTech. https://doi.org/10.5772/12929

Wetser, K., Sudirjo, E., Buisman, C. J. N., & Strik, D. P. B. T. B. (2015). Electricity generation by a plant microbial fuel cell with an integrated oxygen reducing biocathode. *Applied Energy*, 137, 151–157. https://doi.org/10.1016/j.apenergy.2014.10.006

Widharyanti, I. D., Hendrawan, M. A., & Christwardana, M. (2021). Membraneless Plant Microbial Fuel Cell using Water Hyacinth (Eichhornia crassipes) for Green Energy Generation and Biomass Production. *International Journal of Renewable Energy Development,* 10(1), 71–78. https://doi.org/10.14710/ijred.2021.32403

Zingbe, E., Kongnine, D. M., Agbomahena, B. M., Kpelou, P., & Mouzou, E. (2025). Influence of Coconut Husk Biochar and Inter-Electrode Distance on the No-Load Voltage of the Cymbopogan citratus Microbial Plant Fuel Cell in a Pot. *Electrochem*, 6(1), 9. https://doi.org/10.3390/electrochem6010009